

Analysis of Higgs Self-coupling with ZHH at ILC

Yosuke Takubo

Department of Physics, Tohoku University, Sendai, Japan

Measurement of the cross-section of $e^+e^- \rightarrow ZHH$ offers the information of the trilinear Higgs self-coupling, which is important to confirm the mechanism of the electro-weak symmetry breaking. Since there is huge background in the signal region, background rejection is key point to identify ZHH events. In this paper, we study the possibility to observe the ZHH events at ILC by using $ZHH \rightarrow \nu\bar{\nu}HH/q\bar{q}HH$ events.

1 Introduction

In the standard model, particle masses are generated through the Higgs mechanism. This mechanism relies on a Higgs potential, $V(\Phi) = \lambda(\Phi^2 - \frac{1}{2}v^2)^2$, where ϕ is an iso-doublet scalar field, and v is the vacuum expectation value of its neutral component ($v \sim 246$ GeV). Determination of the Higgs boson mass, which satisfies $m_H^2 = 2\lambda v^2$ at tree level in the standard model, will provide an indirect information about the Higgs potential and its self-coupling, λ_{HHH} . The measurement of the trilinear self-coupling, $\lambda_{HHH} = 6\lambda v$, offers an independent determination of the Higgs potential shape and the most decisive test of the mechanism of the electro-weak symmetry breaking.

λ_{HHH} can be extracted from the measurement of the cross-section for the Higgsstrahlung process (σ_{ZHH}), $e^+e^- \rightarrow ZHH$. For a Higgs mass of 120 GeV, the W fusion process is negligible at $\sqrt{s} = 500$ GeV. Figure 1 shows the relevant Feynman diagrams for this process. The information of λ_{HHH} is included in the diagram of Fig. 1(a), and the relation between the cross-section of ZHH and λ_{HHH} is characterized by $\frac{\Delta\lambda_{HHH}}{\lambda_{HHH}} \sim 1.75 \frac{\Delta\sigma_{ZHH}}{\sigma_{ZHH}}$, where $\Delta\lambda_{HHH}$ and $\Delta\sigma_{ZHH}$ are measurement accuracy of λ_{HHH} and σ_{ZHH} , respectively [1]. For that reason, precise measurement of the cross-section for the ZHH production is essential to determination of the strength of the trilinear Higgs self-coupling.

We have studied the feasibility for observation of ZHH events at the ILC. For the analysis, we assumed a Higgs mass of 120 GeV, $\sqrt{s} = 500$ GeV, and an integrated luminosity of 2 ab^{-1} . The final states of the ZHH production can be categorized into 3 types, depending on the decay modes of Z : $ZHH \rightarrow q\bar{q}HH$ (135.2 ab^{-1}), $ZHH \rightarrow \nu\bar{\nu}HH$ (38.8 ab^{-1}), and $ZHH \rightarrow \ell\bar{\ell}HH$ (19.8 ab^{-1}), where the cross-sections were calculated without the beam polarization, initial-state radiation, and beamstrahlung. In this paper, we report status of the analysis with $ZHH \rightarrow \nu\bar{\nu}HH/q\bar{q}HH$ events.

2 Simulation tools

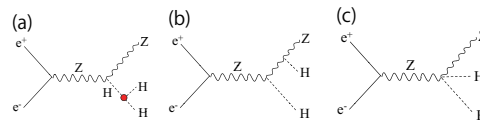


Figure 1: The relevant Feynman diagrams for the ZHH production. The trilinear self-coupling is included in (a).

We have used MadGraph [2] to generate $ZHH \rightarrow \nu\bar{\nu}HH/q\bar{q}HH$ and $t\bar{t}b$ events, where top quarks in $t\bar{t}b$ events are decayed by using DECAY package in MadGraph. $ZZ \rightarrow b\bar{b}b\bar{b}$, tt , and ZH events have been generated by PhysSim [3]. In this study, the beam polarization, initial-state radiation, and beamstrahlung have not been included in the event generations. We also have ignored the finite crossing angle between the electron and positron beams. In both event generations, helicity amplitudes were calculated using the HELAS library [4], which allows us to deal with the effect of gauge boson polarizations properly. Phase space integration and the generation of parton 4-momenta have been performed by BASES/SPRING [5]. Parton showering and hadronization have been carried out by using PYTHIA6.4 [6], where final-state tau leptons are decayed by TAUOLA [7] in order to handle their polarizations correctly.

The generated Monte Carlo events have been passed to a detector simulator called JSFQuickSimulator, which implements the GLD geometry and other detector-performance related parameters [8]. Figure 2 shows a typical event display of $ZHH \rightarrow \nu_\mu\bar{\nu}_\mu HH$.

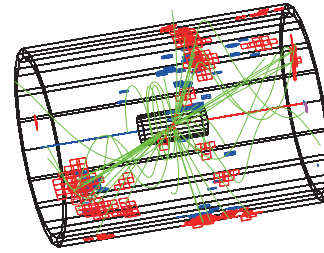


Figure 2: A typical event display of $ZHH \rightarrow \nu_\mu\bar{\nu}_\mu HH$.

3 Analysis

3.1 $ZHH \rightarrow \nu\bar{\nu}HH$

For the Higgs mass of 120 GeV, the Higgs boson mainly decays into $b\bar{b}$ (76% branching ratio in MadGraph). Therefore, we concentrated on $ZHH \rightarrow \nu\bar{\nu}b\bar{b}b\bar{b}$ from $\nu\bar{\nu}HH$ events. As background events, we considered $ZZ \rightarrow b\bar{b}b\bar{b}$ (9.05 fb), tt (583.6 fb), ZH (62.1 fb), and $t\bar{t}b$ (1.2 fb). They have much larger cross-sections than ZHH , necessitating powerful background rejection.

The clusters in the calorimeters are combined to form a jet if the two clusters satisfy $y_{ij} < y_{cut}$, where y_{ij} is y -value of the two clusters. All events are forced to have four jets by adjusting y_{cut} . Then, mass of the Higgs boson was reconstructed to identify $\nu\bar{\nu}HH$ events by minimizing χ^2 value defined as

$$\chi^2 = \frac{(\text{rec} M_{H1} - \text{true} M_H)^2}{\sigma_{H1}^2} + \frac{(\text{rec} M_{H2} - \text{true} M_H)^2}{\sigma_{H2}^2}, \quad (1)$$

where $\text{rec} M_{H1,2}$, $\text{true} M_{H1,2}$, and $\sigma_{H1,2}$ are the reconstructed Higgs mass, the true Higgs mass (120 GeV), and the Higgs mass resolution, respectively. $\sigma_{H1,2}$ was evaluated for each reconstructed Higgs boson by using $31\%/\sqrt{E_{\text{jet}}}$, where E_{jet} is the jet energy. Figure 3 shows the distribution of the sum of the two reconstructed Higgs boson masses for $\nu\bar{\nu}HH$ and background events.

To identify the signal events from the backgrounds, we applied the following selection cuts. We required $\chi^2 < 20$ and $95 \text{ GeV} < M_{H1,2} < 125 \text{ GeV}$ to select events, for which the

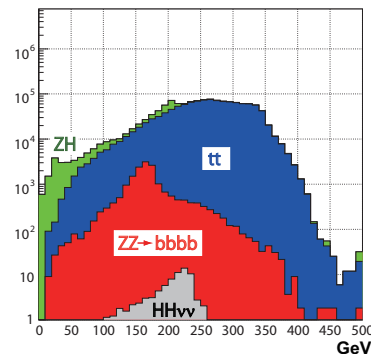


Figure 3: Distribution of the sum of the two reconstructed Higgs masses for $\nu\bar{\nu}HH$ and background events.

Higgs bosons could be well reconstructed. Since Higgs mainly decay into a b -quark pair, the reconstructed mass distribution have a tail in lower mass region due to missing energy by neutrinos from decay processes of the b -quark. For that reason, the mass cut is applied asymmetrically against the Higgs mass. Then, since a Z boson is missing in $\nu\bar{\nu}HH$ events, we set the selection cut on the missing mass ($^{\text{miss}}M$): $90 \text{ GeV} < ^{\text{miss}}M < 170 \text{ GeV}$.

The angular distribution of the particles reconstructed as the Higgs bosons has a peak at $\cos\theta = \pm 1$ for ZZ events whereas the distribution becomes more uniform in $\nu\bar{\nu}HH$ events. We applied the angular cut of $|\cos\theta_{H1,2}| < 0.9$ to reject these ZZ events.

The 4-jet events from ZH events have small missing transverse momentum ($^{\text{miss}}P_T$), which contaminate in the signal region. For that reason, we required $^{\text{miss}}P_T$ above 50 GeV.

After the selection cuts so far, the dominant background was tt events. The leptonic decay mode of W from $t \rightarrow bW$ can be rejected by indentifying isolated charged leptons.

We define the energy deposit within 20 degree around a track as E_{20} . The isolated lepton track was defined to be a track with $10 \text{ GeV} < E_{20} < \frac{2}{11}E_{\text{trk}} - 1.8 \text{ GeV}$, where E_{trk} is energy of the lepton track. We required the number of isolated lepton tracks (N_{lepton}) to be zero.

Finally, the flavor tagging was applied. We identified a jet as a b -jet, when it has 2 tracks with 3-sigma separation from the interaction point. Figure 4 shows the distribution of the number of jets tagged as b -jets after the selection cuts ($N_{b\text{-tag}}$). Since the Higgs boson decays into $b\bar{b}$ with a 76% branching ratio, $\nu\bar{\nu}HH$ events have a peak at $N_{b\text{-tag}} = 4$, whereas tt events have a peak at 2. To reject the tt events effectively, we selected events with $N_{b\text{-tag}} = 4$.

Figure 6 shows the distribution of the sum of the two reconstructed Higgs masses for $ZHH \rightarrow \nu\bar{\nu}HH$ after all the selection cuts. We summarize the reduction rate by each selection cut in Table 2. Finally, we obtained 7.3 events for $\nu\bar{\nu}HH$ and 69.2 events for backgrounds. This result corresponds to a signal significance of 0.8 ($= 7.3/\sqrt{7.3 + 69.2}$). For observation of the ZHH production, further background rejection, especially tt events, is necessary.

3.2 $ZHH \rightarrow q\bar{q}HH$

For the analysis of $qqHH$, all the events are reconstructed as 6-jet events, adjusting the y -value. Here, we considered tt and $t\bar{t}b$ events as background events. The masses of the

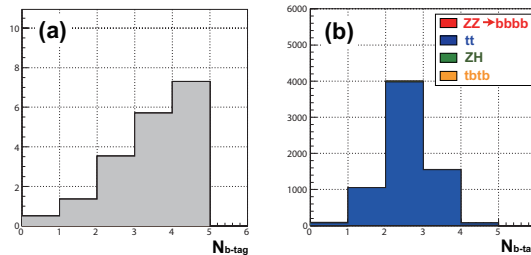


Figure 4: Distribution of the number of jets tagged as b -jets after the selection cuts for $\nu\bar{\nu}HH$ (a) and backgrounds (b).

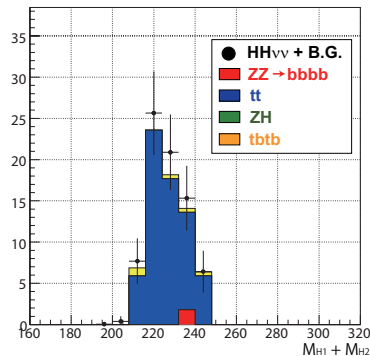


Figure 5: Distribution of the sum of the two reconstructed Higgs boson masses for $ZHH \rightarrow \nu\bar{\nu}HH$ after all the selection cuts.

	$\nu\bar{\nu}HH$	$ZZ \rightarrow bbbb$	tt	ZH	$tbtb$
No cut	77.6	18,100	1,167,200	124,200	2,154
$\chi^2 < 20$	43.7	12,169	364,921	83,065	468
$95 \text{ GeV} < M_{H1,2} < 125 \text{ GeV}$	29.5	387	70,557	8,570	82
$90 \text{ GeV} < M_{\text{miss}} < 170 \text{ GeV}$	26.2	127	32,570	696	45
$ \cos \theta_{H1,2} < 0.9$	23.0	34.4	26,521	447	37
$^{\text{miss}}P_T > 50 \text{ GeV}$	18.4	3.6	17,591	137	25
$N_{\text{lepton}} = 0$	17.8	3.6	6,708	37.3	9.7
$N_{\text{b-tag}} = 4$	7.3	1.8	65	0	2.4

Table 1: Cut statistics.

Higgs and Z boson were reconstructed by minimizing χ^2 value defined as

$$\chi^2 = \frac{(\text{rec } M_{H1} - \text{true } M_H)^2}{\sigma_{H1}^2} + \frac{(\text{rec } M_{H2} - \text{true } M_H)^2}{\sigma_{H2}^2} + \frac{(\text{rec } M_Z - \text{true } M_Z)^2}{\sigma_Z^2}, \quad (2)$$

where $\text{rec } M_{H1,2}$, $\text{rec } M_Z$, $\text{true } M_{H1,2}$, and $\text{true } M_Z$ are the reconstructed Higgs and Z mass and the true Higgs and Z mass, respectively. $\sigma_{H1,2}$ and σ_Z are the Higgs and Z mass resolution, respectively, which are defined in Sec 3.1.

We required $\chi^2 < 20$, $90 \text{ GeV} < M_{H1,2} < 150 \text{ GeV}$, and $60 \text{ GeV} < M_Z < 120 \text{ GeV}$ to select events, for which the Higgs and Z bosons could be well reconstructed. Then, the isolated lepton track was searched to identify the lepton tracks from decay of top quarks in tt and $tbtb$ events. We required the number of isolated lepton tracks (N_{lepton}) to be zero. Since the missing energy of the signal is smaller than tt and $tbtb$ events, $^{\text{miss}}E < 70 \text{ GeV}$ was required. Finally, we applied the b-tagging whose requirement is the same as the analysis for $\nu\bar{\nu}HH$ events. Here, we required that all the jets are b-jets, $N_{\text{b-tag}} = 6$.

After all the cut, we obtained 4.6 events for $qqHH$ and 0.6 events for the background. That corresponds to the signal significance of 2.0 ($= 4.6/\sqrt{4.6+0.6}$). The number of the events at each selection cut is summarized in Table 2.

4 Summary

$ZHH \rightarrow \nu\bar{\nu}HH/q\bar{q}HH$ processes were studied to investigate the possibility of the trilinear Higgs self-coupling at the ILC. In this study, we assumed the Higgs boson mass of 120 GeV, $\sqrt{s} = 500 \text{ GeV}$, and the integrated luminosity of 2 ab^{-1} . After the selection cuts, the signal significance of 0.8 and 2.0 was obtained for $\nu\bar{\nu}HH$ and $q\bar{q}HH$ events, respectively. To extract the information of λ_{HHH} , we must improve the flavor tagging to reject background events effectively.

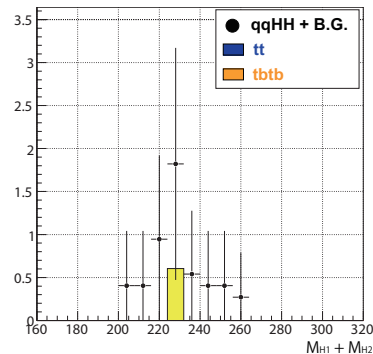


Figure 6: Distribution of the sum of the two reconstructed Higgs boson masses for $ZHH \rightarrow q\bar{q}HH$ after all the selection cuts.

	$qqHH$	tt	$t\bar{t}\bar{t}b$
No cut	270	1,167,200	124,200
$\chi^2 < 20$	219	615,456	1,810
$90 \text{ GeV} < M_{H_{1,2}} < 150 \text{ GeV}$	214	600,899	1,781
$60 \text{ GeV} < M_Z < 120 \text{ GeV}$	213	595,533	1,771
$N_{\text{lepton}} = 0$	193	467,154	1,240
$\text{miss } E < 70 \text{ GeV}$	170	352,061	943
$N_{\text{b-tag}} = 6$	4.6	0	0.6

Table 2: Cut statistics.

5 Acknowledgments

The authors would like to thank all the members of the ILC physics subgroup [9] for useful discussions. This study is supported in part by the Creative Scientific Research Grant No. 18GS0202 of the Japan Society for Promotion of Science, and Dean's Grant for Exploratory Research in Graduate School of Science of Tohoku University.

References

- [1] C. Castanier, P. Gay, P. Lutz, J Orloff, arXiv:hep-ex/0101028.
- [2] <http://madgraph.hep.uiuc.edu/>.
- [3] <http://acfahep.kek.jp/subg/sim/softs.html>.
- [4] H. Murayama, I. Watanabe, K. Hagiwara, KEK-91-11, (1992) 184.
- [5] T. Ishikawa, T. Kaneko, K. Kato, S. Kawabata, *Comp, Phys. Comm.* **41** (1986) 127.
- [6] T. Sjöstrand, *Comp, Phys. Comm.* **82** (1994) 74.
- [7] <http://wasm.home.cern.ch/wasm/goodies.html>.
- [8] GLD Detector Outline Document, arXiv:physics/0607154.
- [9] <http://www-jlc.kek.jp/subg/physics/ilcphys/>.